# Inverse Sensitivity in Plasmonic Nanosensors via Enzyme-Guided Crystal Growth

Laura Rodríguez-Lorenzo,[2] Roberto de la Rica,[1,*] Ramón Álvarez-Puebla,[2] Luis M. Liz-Marzán,[2] Molly M. Stevens[1,*]

[1]Department of Materials, Department of Bioengineering and Institute for Biomedical Engineering, Imperial College London, Exhibition Road, London, SW7 2AZ (UK)

[2]Departamento de Quimica Fisica and Unidad Asociada CSIC, Universidade de Vigo, 36310, Vigo (Spain)

* m.stevens@imperial.ac.uk

* roberto.delarica@gmail.com

Nature Materials 11, 604–607 (2012) doi:10.1038/nmat3337

**Lowering the limit of detection is a fundamental aspect in the design of sensors important to food safety regulations,[1-2] environmental policies[3-5] and the diagnosis of severe diseases.[6-10] However, conventional transducers generate a signal that is directly proportional to the concentration of the target molecule. As such, the presence of chemical species at ultralow concentrations results in tiny variations in the physical properties of the sensor and these are difficult to detect with confidence. Here we redefine the limit of detection of nanoparticle sensors by presenting a signal generation mechanism that induces a larger signal when the target molecule is less concentrated. The key step to achieve this inverse sensitivity is to use an enzyme in order to control the rate of nucleation of silver nanocrystals on plasmonic transducers. The outstanding sensitivity and robustness of this approach was demonstrated by detecting the cancer biomarker prostate specific antigen (PSA) down to $10^{-18}$ g·mL$^{-1}$ ($4 \cdot 10^{-20}$ M) in whole serum.**

Metal nanoparticles are outstanding building blocks for the fabrication of biosensors when their surface plasmon resonance (LSPR) shifts in response to a biorecognition event.[11] In these detection platforms, the largest variations in the LSPR are observed when another metallic nanostructure interacts in close proximity with the nanosensor. We have evolved this concept by generating silver nanostructures *in situ* that tailor the LSPR of gold nanosensors. In our approach, the LSPR is tuned by programming crystal growth to favor either the formation of a silver coating around the transducer or the nucleation of silver nanocrystals in solution, as depicted in Figure 1. To control crystal growth we use the enzyme glucose oxidase (GOx), which generates hydrogen peroxide that reduces silver ions around gold nanosensors,[12] in our case gold nanostars.[13] Enzymes have been previously shown to work as nanoreactors that generate nanostructures of controlled size by limiting the rate of nucleation of the nascent nanocrystals.[14,15] Here, GOx determines the rate of crystallization of silver to

favor either the nucleation or the growth of the nanocrystals , and this phenomenon is utilized to tailor the plasmonic response of the nanoparticle sensors. When the enzyme is present at low concentrations, the short supply of reducing agent dictates slow crystal growth conditions. This favors the growth of a homogeneous silver coating on the gold nanostars as seeding points,[16] which yields a blue shift in the LSPR of the nanosensors.[17,18] However, when the concentration of GOx is high, the abundant reducing agent favors nucleation instead of epitaxial growth and free-standing silver nanocrystals are obtained.[16] Consequently, less silver is deposited on the nanosensors and the LSPR shifts less than in the presence of GOx at low concentrations. To apply this phenomenon as a universal tool for biosensing, GOx can be bound to antibodies and used as the label in a classical enzyme-linked immunoassay. Since the concentration of GOx is directly related to the concentration of the analyte via immunoreaction, the presence of the target molecule at low concentrations is expected to yield a larger variation of the optical properties of the plasmonic transducers via the formation of a silver coating. This inverse relationship between concentration and signal hereby referred as "inverse sensitivity" makes this approach highly suitable for the fabrication of ultrasensitive sensors because the signal generated by the analyte at low concentrations is the highest, making it is easy to differentiate it from false signals originating from non-specific interactions.

Figure 2a shows a high-resolution transmission electron microscopy (HRTEM) image of gold nanostars used as plasmonic transducers of GOx activity. The high aspect ratio spikes localize the low energy plasmon mode at their tips, which results in a dominant LSPR band in the near infrared region (Figure 2b).[19,20] To test the signal generation mechanism depicted in Figure 1, gold nanostars were covalently modified with GOx (see Section S1 in the Supplementary Information). After adding glucose to trigger the enzymatic production of hydrogen peroxide, silver nitrate was added to initiate crystal growth. In Figure 2b (green

curve), the LSPR of gold nanostars modified with $10^{-14}$ g·mL$^{-1}$ GOx undergoes a blue shift after silver reduction, as expected from the formation of a silver coating around gold nanosensors.[13, 17-18] The same experiment performed with gold nanostars modified with a non-catalytic globular protein (BSA) does not alter the optical properties of the nanosensors (blue curve), which indicates that the presence of GOx is essential for the formation of a silver coating. The modification of the nanosensors with as low as $10^{-20}$ g·mL$^{-1}$ GOx yields a drastic change in the optical properties of the nanoparticle solution that is much larger than the one obtained with $10^{-14}$ g·mL$^{-1}$ GOx (red curve). Figure 2c (red circles) represents the shift of the LSPR band position as a function of GOx concentration, which clearly shows that the shift increases when the concentration of GOx decreases in the range between $10^{-13}$ and $10^{-20}$ g·mL$^{-1}$. Higher concentrations of GOx do not result in a further shift of the LSPR absorbance band. Conversely, control experiments performed with the same GOx-modified nanostars but without adding the enzyme substrate glucose have a negligible effect on the optical properties of the nanosensors (black circles). This result, along with the absence of signal in the experiment in the presence of glucose but in the absence of GOx (Fig. 2b), demonstrates that the production of hydrogen peroxide by the biocatalytic activity of the enzyme is the key factor for the reduction of silver ions.

In the signal generation mechanism depicted in Figure 1, the magnitude of the signal registered by plasmonic nanosensors depends on the rate of crystallization, which favors either the growth of a silver coating on the existing nanocrystals or the nucleation of free-standing small particles. To demonstrate this theory, the presence of silver nanostructures in the solutions containing GOx-modified nanostars was determined after the crystal growth step. Figures 3a and 3b show representative HRTEM images obtained after silver reduction in the presence of $10^{-20}$ g·mL$^{-1}$ and $10^{-14}$ g·mL$^{-1}$ GOx, respectively. Free-standing quasi-spherical nanoparticles were observed in abundance when the nanostars were modified with

$10^{-14}$ g·mL$^{-1}$ GOx, and these nanoparticles were found to be made of silver (Section S4 of the Supplementary Information). In Figures 3c and 3d, X-ray energy dispersive spectroscopy (XEDS) maps demonstrate the presence of a uniform silver coating around Au nanostars modified with $10^{-14}$ g·mL$^{-1}$ GOx. Coatings containing on average 4 % more silver were observed around nanostars modified with $10^{-20}$ g·mL$^{-1}$ GOx, which is in agreement with the larger LSPR shift observed in Fig. 2b. These observations agree with the proposed mechanism that low concentrations of reducing agent result in a slow rate of crystallization, which in turn favors the epitaxial growth of a silver coating on gold seeds, as schematically shown in Figure 1. These silver coatings shift the LSPR of the gold nanostars by as much as 150 nm, as shown in Figure 2b. This effect is due to the hybridization of the dielectric constants of gold and silver in these segregated nanoalloys. The dielectric function of silver has a larger imaginary part than that of gold, which means that it is more absorptive.[21] By contrast, high concentrations of reducing agent favor the nucleation of free-standing nanoparticles (Fig. 3b). Under these conditions, the lower amount of silver around the nanostars shifts the LSPR by only 80 nm, as shown in Figure 2b. These experiments confirm that the growth of silver on the nanosensors is responsible for the blue shift observed in the LSPR, and that the inverse sensitivity recorded at different enzyme concentrations originates from harnessing crystal growth to favor either the nucleation or the growth of silver nanostructures, as depicted in Figure 1.

After demonstrating the mechanism of signal generation via enzyme-guided crystal growth, we designed an experiment to prove the extreme sensitivity and robustness of plasmonic nanosensors when working in the inverse sensitivity regime. Gold nanostars modified with polyclonal antibodies against prostate specific antigen (PSA) captured this cancer biomarker, which was then detected with monoclonal antibodies and labeled with secondary antibodies bound to GOx. PSA was chosen as the model analyte because the detection of this biomarker

at ultralow concentrations is crucial for the early diagnosis of cancer recurrence in patients that have undergone total prostatectomy, which makes it an interesting clinical target for testing ultrasensitive sensors.[22] Moreover, the detection of PSA in human serum provides a complex matrix to prove the robustness of these plasmonic nanosensors against interferences. In Figure 4a the calibration curve for the detection of PSA in buffered solution shows the negative slope that is characteristic of inverse sensitivity (see also Section S5 of the Supplementary Information). The limit of detection, defined here as the lowest concentration of analyte in the inverse sensitivity regime, was $10^{-18}$ g·mL$^{-1}$. Although the signal generation time is longer (ca. 3 h), this result is one order of magnitude lower compared to recently proposed ultrasensitive digital ELISA assays.[7] The same experiments performed with a control protein did not yield any significant signal, which proved that the effect of non-specific interactions between the GOx-labeled antibodies and the nanosensors were minimal (Fig. 4, blue dots). When PSA was spiked into non-diluted human serum, the absolute value of the slope in the calibration curve decreased and the dynamic range was reduced by one order of magnitude. This is attributed to endogenous levels of PSA and non-specific interactions between the antibodies and proteins present in the serum, which increase the concentration of GOx and therefore decrease the signal of the bioassay (see also section S6 in the Supplementary Information). However, the limit of detection did not change and the solution containing PSA at the ultralow concentration of $10^{-18}$ g·mL$^{-1}$ still yielded the highest signal, therefore demonstrating the suitability of this approach for the detection of minute concentrations of target proteins in complex matrices such as body fluids.

The inverse sensitivity phenomenon reported here was possible by controlling the kinetics of crystal growth with an enzyme, which in turn determined the signal registered by the transducer. This concept opens up exciting new possibilities for biosensing when the rich chemistry of crystal growth is merged with the outstanding physical properties of

nanosensors. In such detection schemes, the alteration of key parameters of the growth solution such as pH, concentration of precursors and presence of capping agents can exert a huge impact on the size,[23] morphology,[24,25] crystallinity,[26,27] and degree of aggregation of nanocrystals,[29-30] all of which are crucial factors that can modulate the response of the transducer.

## METHODS

### Signal generation via enzyme-guided crystal growth

The synthesis of Au nanostars has been reported elsewhere.[19] Briefly, nanostars were prepared by adding PVP-coated gold seeds ([Au] = 9.29 $10^{-4}$ M) in ethanol to a mixture of $HAuCl_4$ (2.73 $10^{-4}$ M) and poly(vinylpyrrolidone) (PVP, 10 mM) in DMF under rapid stirring at room temperature. The prepared nanostars have an average total size of 60 ± 8 nm. Protocols for covalent attachment of biomolecules to PVP-stabilized gold nanostars can be found in Section S1 of the Supplementary Information. The protein-modified nanosensors are stable in solutions containing highly concentrated electrolytes as shown in Section S2 of the Supplementary Information. The production of $H_2O_2$ was initiated by adding glucose (100 mM) to GOx-modified nanostars in MES buffer (10 mM, pH 5.9) for 1 h. Subsequently, $AgNO_3$ (0.1 mM) and $NH_3$ (40 mM) were added to trigger the reduction of silver ions on the gold nanosensors. Spectral changes were measured with a Jasco V-670 UV-vis-NIR spectrophotometer after 2 h. High resolution (HRTEM) and scanning transmission electron microscopy (STEM) images were obtained with a JEOL JEM 2010 FEG-TEM microscope operating at an acceleration voltage of 200 kV. The samples were prepared by depositing a droplet on carbon-coated grids and evaporating the solvent in air at room temperature. X-ray energy dispersive spectra (XEDS) were acquired using an Inca Energy 200 TEM system from

Oxford Instruments, and elemental mapping was acquired by coupling the X-ray spectrometer to a STEM unit, equipped with a high angle annular dark field (HAADF) detector. Mapping was performed with a 0.7 nm probe size, and the acquisition time was limited to 60 s to avoid sample drift. The corresponding quantitative EDS measurements were performed using an INCA EDS microanalysis system from Oxford Instruments. Determination of the relative amount of silver in the coatings was carried by standardless analysis using the Cliff-Lorimer correction with absorbance. Calculations were performed on three different sites on the grid.

**PSA detection with antibody-modified gold nanostars**

The conjugation of GOx to anti-mouse IgG is described in Section S3 of the Supplementary Information. To detect PSA, gold nanostars were modified with polyclonal anti-PSA raised in rabbit (Abcam) as detailed in Section S1 of the Supplementary Information. Then, the antibody-modified gold nanostars ([Au] = 0.25 mM) were incubated with PSA (Sigma) in the concentration range between $10^{-19}$ and $10^{-12}$ g·mL$^{-1}$ in a final volume of 1 mL for 2 h. PSA samples were obtained by diluting a concentrated solution either in PBS or in whole serum from a female donor (Sera Lab). This serum was found to contain endogenous PSA with the concentration of ca. $10^{-18}$ g·mL$^{-1}$ (see also section S6 in the Supplementary Information). The particles were then washed by centrifugation (2000 rpm, 10 min) and re-dispersed with PBS. Next, 10 L of monoclonal anti-PSA developed in mouse (0.13 mg·mL$^{-1}$) was added to detect the PSA with a sandwich immunoassay format. After 2 h, the particles were washed and re-dispersed in PBS and 20 L of GOx-labeled anti-mouse IgG added for 2 h at room temperature. After washing once with MES buffer containing Tween-20 (0.05%) and once with MES buffer, the signal generation step was carried out as described above. To demonstrate that the signal was specific and generated by the antibody-antigen recognition,

control experiments were performed by following exactly the same procedure but substituting PSA for bovine serum albumin (BSA) during the analyte incubation step (blue and green dots in Figs. 4a and 4b, respectively).

REFERENCES


1. Batt, C. A. Food Pathogen Detection. *Science* **316**, 1579-1580 (2007)

2. de la Rica, R., Baldi, A., Fernandez-Sanchez, C. & Matsui, H. Single-Cell Pathogen Detection with a Reverse-Phase Immunoassay on Impedimetric Transducers. *Anal. Chem.* **81,** 7732-7736 (2009)

3. Ferber, D. Overhaul of CDC Panel Revives Lead Safety Debate. *Science* **298,** 732-732 (2002)

4. de la Rica, R., Mendoza, E. & Matsui H. Bioinspired Target-Specific Crystallization on Peptide Nanotubes for Ultrasensitive Pb Ion Detection. *Small* **6**, 1753-1756 (2010)

5. Li, D., Wieckowska, A. & Willner, I. Optical analysis of Hg(2+) ions by oligonucleotide-gold-nanoparticle hybrids and DNA-based machines. *Angew. Chem. Int. Ed.* **47**, 3927-3931 (2008)

6. Giljohann D. A. & Mirkin C. A. Drivers of biodiagnostic development. *Nature* **462**, 461-464 (2009)

7. Rissin, D. M. *et al.* Single-molecule enzyme-linked immunosorbent assay detects serum proteins at subfemtomolar concentrations. *Nat. Biotechnol.* **28**, 596-599 (2010)

8. Fan, R. *et al.* Integrated barcode chips for rapid, multiplexed analysis of proteins in microliter quantities of blood. *Nat. Biotechnol.* **26**, 1373-1378 (2008)

9. Laromaine, A., Koh, L. L., Murugesan, M., Ulijn, R. V., Stevens, M. M. Protease-triggered dispersion of nanoparticle assemblies. *J. Am. Chem. Soc.* **129**, 4156-4157 (2007)

10. Miranda, O. R. *et al*. Enzyme-Amplified Array Sensing of Proteins in Solution and in Biofluids. *J. Am. Chem. Soc.* **132**, 5285–5289 (2010)

11. Aili, D. & Stevens, M. M. Bioresponsive peptide-inorganic hybrid nanomaterials. *Chem. Soc. Rev.* **39**, 3358-3370 (2010)

12. Willner, I., Baron, R. & Willner, B. Growing Metal Nanoparticles by Enzymes. *Adv. Mater.* **18**, 1109-1120 (2006)

13. Liz-Marzan, L. M. Tailoring Surface Plasmons through the Morphology and Assembly of Metal Nanoparticles. *Langmuir* **22**, 32-41 (2006)

14. Pejoux, C., de la Rica, R. & Matsui, H. Biomimetic Crystallization of Sulfide Semiconductor Nanoparticles in Aqueous Solution. *Small* **6**, 999-1002 (2010)

15. Kisailus, D., Choi, J. H., Weaver, J. C., Yang, W. J. & Morse, D. E. Enzymatic synthesis and nanostructural control of gallium oxide at low temperature. *Adv. Mater.* **17**, 314-318 (2005)

16. Jana, N. R., Gearheart, L. & Murphy, C. J. Evidence for Seed-Mediated Nucleation in the Chemical Reduction of Gold Salts to Gold Nanoparticles. *Chem. Mater.* **13**, 2313-2322 (2001)

17. J. T. Seo *et al*. Optical nonlinearities of Au Nanoparticles and Au/Ag coreshells. *Opt. Lett.* **34**, 307-309 (2009)

18. Cardinal, M. F., Rodriguez-Gonzalez, B., Alvarez-Puebla, R. A., Perez-Juste, J., Liz-Marzan, L. M. Modulation of Localized Surface Plasmon and SERS response in Gold Dumbbells thorugh Silver Coating. *J. Phys. Chem. C.* **114**, 10417-10423 (2010)

19. Kumar, P. S., Pastoriza-Santos, I., Rodriguez-Gonzalez, B., Garcia de Abajo, F. J. & Liz-Marzan, L. M. High-yield synthesis and optical response of gold nanostars. *Nanotechnology* **19**, 015606 (2007)

20. Barbosa, S. *et al.* Tuning Size and Sensing Properties in Colloidal Gold Nanostars. *Langmuir* **26**, 14943-14950 (2010)

21. Liu, M. & Guyot-Sionnest, P. Mechanism of Silver(I)-assisted Growth of Gold Nanorods and Bipyramids. *J. Phys. Chem. B* **109**, 22192–2220 (2005)

22. Thaxton, C. S. *et al.* Nanoparticle-based bio-barcode assay redefines ‘‘undetectable’’ PSA and biochemical recurrence after radical prostatectomy. *Proc. Natl. Acad. Sci. USA* **106**, 18437-18442 (2009)

23. Sanchez-Iglesias, A. *et al.* Synthesis and optical properties of gold nanodecahedra with size control. *Adv. Mater.* **18**, 2529-2534 (2006)

24. Roh, K.-H., Martin, D. C. & Lahann, J. Biphasic Janus particles with nanoscale anisotropy. *Nat. Mater.* **4**, 759 - 763 (2005)

25. Marinakos, S. M., Chen, S. & Chilkoti, A. Plasmonic Detection of a Model Analyte in Serum by a Gold Nanorod Sensor. *Anal. Chem.* **79**, 5278-5283 (2007)

26. de la Rica, R. & Matsui, H. Urease as a nanoreactor for growing crystalline ZnO nanoshells at room temperature. *Angew. Chem. Int. Ed.* **47**, 5415-5417 (2008)

27. Kisailus, D., Schwenzer, B., Gomm, J., Weaver, J. C. & Morse, D. E. Kinetically controlled catalytic formation of zinc oxide thin films at low temperature. *J. Am. Chem. Soc.* **128**, 10276-10280 (2006)

28. Tang, Z., Zhang, Z., Wang, Y., Glotzer, S. C., Kotov, N. A. Self-Assembly of CdTe Nanocrystals into Free-Floating Sheets. *Science* **314**, 274-278 (2006)

29. Aili, D., Selegard, R., Baltzer, L., Enander, K. & Liedberg, B. Colorimetric Protein Sensing by Controlled Assembly of Gold Nanoparticles Functionalized with Synthetic Receptors. *Small* **5**, 2445-2452 (2009)

30. DeVries *et al.* Divalent metal nanoparticles. *Science* **315**, 358-361 (2007)

## ACKNOWLEDGEMENTS

Dr. B. Rodríguez-González is thanked for electron microscopy analysis. M.M.S. thanks the EPSRC and ERC starting investigator grant “Naturale” for funding. This research was supported by a Marie Curie Intra European Fellowship within the 7th European Community Framework Programme (R.R.). L.M.L.-M. acknowledges the ERC grant “Plasmaquo” for funding. L.R.-L. acknowledges an FPU scholarship from Ministerio de Educación, Spain. R.A.A.-P. acknowledges financial support from the Ramon y Cajal Program (Ministerio de Ciencia e Innovación, Spain).

## AUTHOR CONTRIBUTIONS

R.R elaborated the concept and designed experiments. L. R.-L. performed the experiments. M. M. S. and L. L.-M. supervised the project. All the authors participated in scientific discussions and wrote the paper.

## COMPETING FINANCIAL INTERESTS

The authors declare no competing financial interests

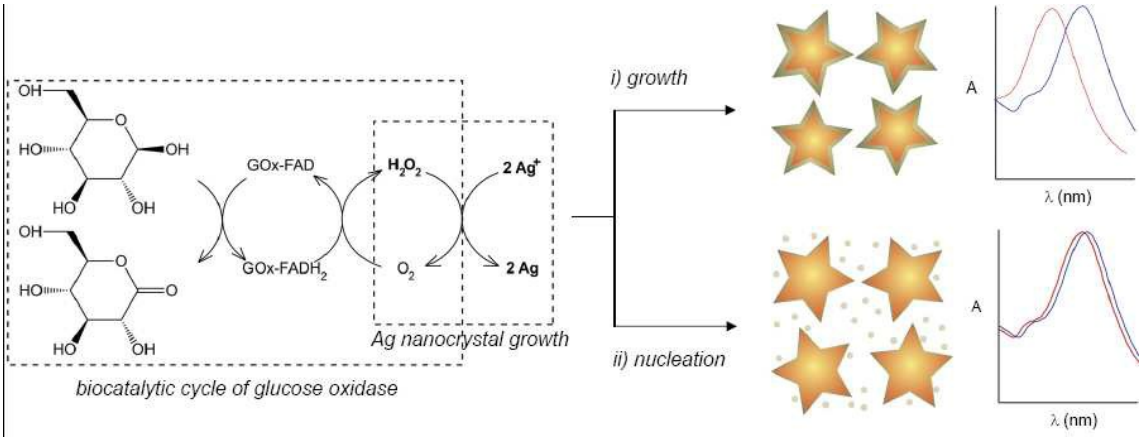


**Figure 1.** Scheme of the proposed signal generation mechanism via enzyme-guided crystal growth. Glucose oxidase (GOx) generates hydrogen peroxide, which reduces silver ions to grow a silver coating around plasmonic nanosensors (gold nanostars); i) at low concentrations of GOx the nucleation rate is slow, which favors the growth of a conformal silver coating that induces a large blue shift in the LSPR of the nanosensors; ii) when GOx is present at high concentrations, the fast crystal growth conditions stimulate the nucleation of Ag nanocrystals and less silver is deposited on the nanosensors, therefore generating a smaller variation of the LSPR. When the concentration of GOx is related to the concentration of a target molecule via

immunoassay, this signal generation step induces inverse sensitivity because condition (i) is fulfilled at low concentrations of analyte.

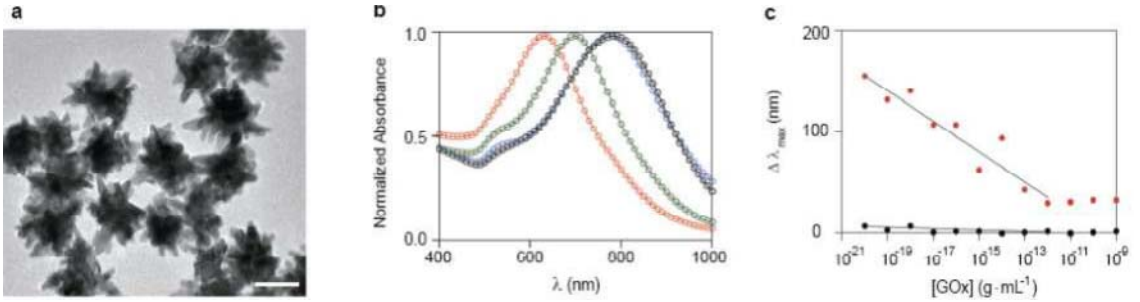


**Figure 2.** Inverse sensitivity in plasmonic nanosensors. a) HRTEM image of gold nanostars (scale bar: 50 nm); b) Vis-NIR spectra of the nanosensors (black), modified with $10^{-14}$ g·mL$^{-1}$ GOx (green), $10^{-20}$ g·mL$^{-1}$ GOx (red) and without GOx (blue) after the signal generation step; c) blue shift of the LSPR absorbance band ( max) as a function of the concentration of GOx in the immobilization solution when the signal generation step is performed in the absence (black) or in the presence (red) of the enzyme substrate glucose (semilogarithmic scale). The spectral shift was calculated with respect to the control experiment in the absence of GOx (blue curve in Fig. 2b).

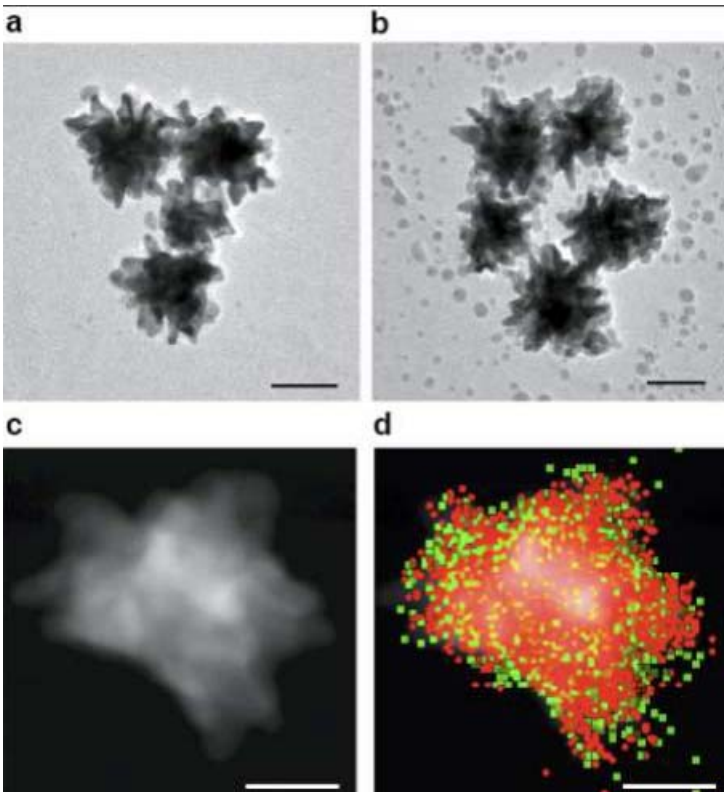


**Figure 3.** HRTEM pictures after the signal generation step when gold nanostars were modified with a) $10^{-20}$ g·mL$^{-1}$ GOx, and b) $10^{-14}$ g·mL$^{-1}$ GOx (scale bar: 50 nm); STEM image (c) and XEDS map (d) showing the distribution of gold (red) and silver (green) around nanostars modified with $10^{-14}$ g·mL$^{-1}$ GOx (scale bar: 20 nm). XEDS spectra are shown in Section S4 of the Supplementary Information.

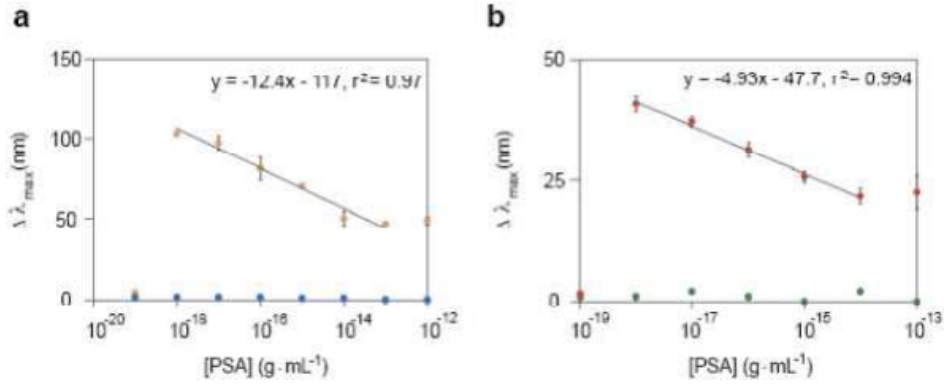

**Figure 4.** Immunoassay for the ultrasensitive detection of PSA with GOx-labeled antibodies. Blue shift of the LSPR absorbance band ( max) as a function of the concentration of: a) PSA in PBS (orange) and BSA in PBS (blue), b) PSA spiked into whole serum (red) and BSA spiked into whole serum (green). Error bars are the standard deviation (n = 3). The spectral shift was calculated with respect to the control experiment in the absence of the analyte (see section S5 in the Supplementary Information)